Protective effect of calycosin-7-O-β-D-glucopyranoside against oxidative stress of BRL-3A cells induced by thioacetamide

Li Jian, Lin Xin, Ma Yufang, Huang Yifan

University Key Laboratory for Integrated Chinese Traditional and Western Veterinary Medicine and Animal Healthcare in Fujian Province, Fujian Agriculture and Forestry University, Fuzhou, China

Submitted: 21-08-2014 Revised: 26-09-2014 Published: 10-07-2015

ABSTRACT

Background: Calycosin-7-O-β-D-glucopyranoside (CG) is a natural isoflavone found in traditional Chinese medicines Astragali Radix (AR). **Objective:** Calycosin-7-O-β-D-glucopyranoside, an isoflavone isolated from AR, has been found to have potent antioxidantive effects. This study was designed to investigate whether CG prevents oxidative stress induced by thioacetamide (TAA). **Materials and Methods:** BRL-3A cells were pretreated with different concentrations of CG (10, 20, 40 mg/mL) for 12 h and then exposed to 0.18 mol/L TAA for 2 h. The cell viability were examined by 3-[4,5-dimethylthiazol-2-yl]-2,5 diphenyl-tetrazolium assay, total antioxidant capacity, malondialdehyde (MDA) and the activity of antioxidant enzymes, including catalase, glutathione peroxidase and superoxide dismutase were determined by microplate method. Reactive oxygen species (ROS) generation was quantified by the 2′,7′-dichlorofluorescin-diacetate method. Protein and mRNA expression of CYP2E1 were determined by western blotting and real-time PCR. **Results:** The cell oxidative stress was significantly increased after 2 h of TAA exposure. Pretreatment of BRL-3A cells with CG significantly increased the activities of antioxidant enzymes, scavenged ROS and reduced MDA production. CG decreased the expression of CYP2E1, and ultimately decreased TAA-induced BRL-3A cells oxidative stress. **Conclusions:** Calycosin-7-O-β-D-glucopyranoside has a protective effect against TAA-induced oxidative stress in BRL-3A cells, and that the underlying mechanism involves in scavenging of ROS and the modulating expression of CYP2E1.

Key words: BRL-3A cell, calycosin-7-O-β-D-glucopyranoside, CYP2E1, oxidative stress, thioacetamide

Access this article online

Website: www.phcog.com

DOI: 10.4103/0973-1296.160461

Quick Response Code:

Chemical compounds studied in this article: Calycosin-7-O-β-D-glucopyranoside (PubChem CID: 5318267), thioacetamide (PubChem CID: 2723949), Bifendate (PubChem CID: 108213).

INTRODUCTION

Liver is the most important detoxification organ, and many xenobiotics are metabolized in it. These metabolic processes often lead to liver damage in varying degrees, which resulted in the internal environment disorders of the body. Increasing evidence indicated that oxidative stress is a core process for most types of liver injury.[1,2] Therefore, searching for drugs against liver oxidative stress, has been part of the key ways to treat various types of liver injury.

Astragali Radix (AR), which is the dried root of *Astragalus membranaceus* (Fisch.) Bge.var.*mongholicus* (Bge.) Hsiao or *A. membranaceus* (Fisch.) Bge.,[3] has a long history of medicinal use in traditional Chinese medicines. It has been formulated as an ingredient of herbal mixtures to treat patients with deficiency in vitality, which symptomatically presents with fatigue, diarrhea and lack of appetite.[4] It also has been used in Chinese medicine for the treatment of liver cirrhosis and fibrosis with an excellent safety record.[5,6] Calycosin-7-O-β-D-glucopyranoside [Figure 1] is a natural isoflavone, which is one of the two functional components of AR prescribed in Chinese pharmacopoeia,[3] and its

Address for correspondence:
Dr. Huang Yifan, University Key Laboratory for Integrated Chinese Traditional and Western Veterinary Medicine and Animal Healthcare in Fujian Province, Fujian Agriculture and Forestry University, Fuzhou, China.
E-mail: huangyifanfjnl@sina.com

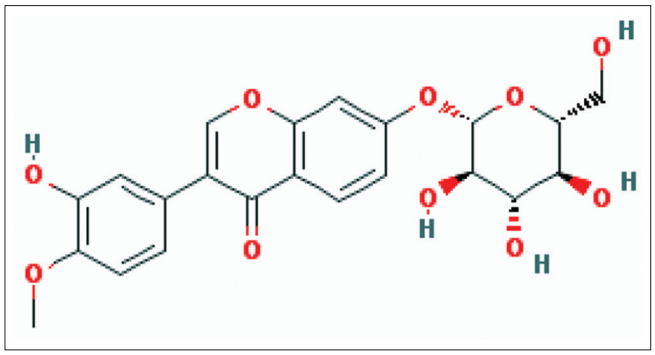

Figure 1: The structure of Calycosin-7-O-β-D-glucopyranoside

hepatoprotective effect has not been reported. Bifendate is a synthetic compound derived from schizandrin C (a component of *Fructus Schizandrae*) that is used in treatment of various liver diseases such as chronic viral hepatitis, chemically or drug induced hepatic injury.[7] And in this study, it was used as the positive control drugs.

Because reactive oxygen species (ROS) are direct products of oxidative stress and CYP2E1 is involved in production of ROS,[8] we investigated the hypothesis that CG attenuate ROS by inhibiting CYP2E1 expression in oxidative stressed BRL-3A cells. The consequence of this report support our hypothesis and provide novel insights into the mechanisms of the antioxidant effect of CG.

MATERIALS AND METHODS

General

BRL-3A immortalized rat hepatocytes were used between passages 10 and 20 (cell resource center of the Shanghai Institute for Biological Science, CAS, catalog number: GNR 10).

Calycosin-7-O-β-D-glucopyranoside was purchased from the Chinese National Institute for the Control of Pharmaceutical and Biological Products (Batch No. 111920-201203). Thioacetamide (TAA), 2',7'-dichlorodihydrofluorescein diacetate (DCFH-DA) and phenylmethanesulfonyl fluoride (PMSF) were purchased from Sigma (USA). DMEM (high glucose) medium and trypsin-ethylenediaminetetraacetic acid were purchased from HyClone (USA). Fetal bovine serum (FBS) was purchased from GE Healthcare Life Sciences (USA). 3-[4,5-dimethylthiazol-2-yl]-2,5 diphenyl-tetrazolium (MTT) and dimethyl sulfoxide (DMSO) were purchased from Solarbio (China). Assay kits for aminotransferase and antioxidant enzyme activities were purchased from Nanjing Jiancheng Bioengineering Institute (China). RNAiso Plus, Primescipt™ RT reagent kit and SYBR® Premix Ex Taq™ were purchased from Takara (China). RIPA lysis buffer, BCA protein assay, and anti-rabbit IgG-HRP antibody were purchased from Pierce (USA). Nitrocellulose membranes and anti-CYP2E1 antibody were purchased from Millipore (USA). Anti-GAPDH antibody was purchased from Cell Signaling (USA). The enhanced chemiluminescence (ECL) detection kit was purchased from Advansta (China). All other chemicals were of analytical grade and commercially available.

Cell cultures and 3-[4,5-dimethylthiazol-2-yl]-2,5 diphenyl-tetrazolium bioassay

BRL-3A cells were cultured in DMEM/high glucose medium supplemented with 10% heat-inactivated FBS, 100 U/mL penicillin and 100 μg/mL streptomycin in a water-saturated atmosphere of 5% CO_2 at 37°C. Cells were seeded in multi-well plates or flasks for 24 h.

BRL-3A cells (2×10^5) were plated in 96-well culture plates in 100 μL of culture medium and incubated at 37°C in humidified 5% CO_2. The day after, 100 μL TAA of different concentrations (0.06, 0.09, 0.12, 0.15, 0.18, 0.21, 0.24 mol/L) was added to the cells and 100 μL culture medium was added to the control group, then incubated for 2 h. Each group has 10 Repetitions. After the treatment, cell viability was assessed through MTT assay.[9] Briefly, a 20 μL of MTT stock solution (5 mg/mL) was added and incubated for 4 h. Then, the supernatants were removed, and the formazan crystals in each well were dissolved in 150 μL of DMSO for quantification at 570 nm with a microplate reader (iMark, Bio-Rad, USA). The cell viability was expressed as a percentage over control.

According to the method above, the cytotoxicity of CG (5, 10, 20, 40, 60, 80, 100 mg/L) and bifendate (1, 10, 20, 30, 40, 50, 60 mg/L) was detected.

Cell grouping and viability

The cells were then divided into six groups to be used to generate a negative control group (NCG), a TAA groups (TAAG), three CG groups with low, medium and high concentration (C1G, C2G and C3G), and a positive control group (PCG). All the BRL-3A cells were seeded in 6-well plates at a density of 2×10^4 cells/well.

Cells of NCG were cultured in normal medium all the time. The cells of TAAG were cultured continually in normal medium for 12 h, the cells of C1G, C2G and C3G were cultured in normal medium supplemented with different concentrations of CG for 12 h, and the cells of PCG were cultured in normal medium supplemented with bifendate for 12 h. At last, in all groups except NCG, cells were then cultured in normal medium supplemented

with TAA for 2 h. The cell viability were detected by MTT assay.

Determination of aminotransferase

BRL-3A cells were cultured and treated according to the above methods. Then the supernatants were collected for determination. Alanine aminotransferase (ALT) and aspartate amino transferase (AST) in cell supernatants were evaluated according to the method of Reitman and Frankel[10] using ELISA kits supplied by Nanjing Jiancheng Bioengineering Institute (China).

Determination of antioxidant profiles and lipid peroxidation

BRL-3A cells were digested with 0.25% trypsin, and then broken with an ultrasonic welder (VCX130, Sonics and Materials, USA). And the antioxidant profiles and lipid peroxidation in the supernatant were determined using assay kits according to the manufacturer's protocol (Nanjing Jiancheng Institute of Biotechnology, Nanjing, China).

Coomassie blue protein binding method[11] was used to determine the protein concentrations using bovine serum albumin as a standard. The analyses of total antioxidant capacity (T-AOC) levels, malondialdehyde (MDA) and total SOD (T-SOD), glutathione peroxidase (GSH-Px) and catalase (CAT) activities were carried out with a UV-Vis spectrophotometer (UV1240, Shimadzu, Japan).

The ferric reducing ability power assay[12] was applied to determine the T-AOC in cells. One unit of T-AOC was equal to 0.01 increases in absorbance of the reaction mixture at 520 nm/mg protein per minute under 37°C incubation and the T-AOC was expressed as U/mg protein. Thiobarbituric acid reaction method[13] was used to determine MDA and the absorbance were read at 530 nm. The MDA content was expressed as nmol/mg protein.

The xanthine oxidase method was used in determining T-SOD activity.[14] One unit is defined as the amount of enzyme needed to exhibit 50% dismutation of the superoxide radical, and enzymatic activity was expressed as U/mg protein.

The rate of enzyme-catalyzed oxidation of GSH per minute assay was applied to determine the activity of GSH-Px[15] and the absorbance was read at 412 nm. The final result was expressed as a decrease of 1.0 μM GSH per 5 min at 37°C after the nonenzymatic reaction was subtracted, and data was expressed as U/mg protein.

The decomposition of H_2O_2 method was used to determine the CAT activity[16] and the absorbance was read at 405 nm. One unit of CAT activity was defined as the amount of CAT required to decompose 1 μmol H_2O_2 per second, and data was expressed as U/mg protein.

Measurement of reactive oxygen species production

The level of intracellular ROS was photographed and quantified by fluorescence with oxidation sensitive dye DCFH-DA[17] in 6-well plates. After the treatment, cells growing at confluency were labeled with 10 μM DCFH-DA in serum-free culture medium DMEM and incubated for 20 min in a CO_2 incubator at 37°C. Nonfluorescent DCFH-DA dye, freely penetrated into cells and got hydrolyzed by intracellular esterase to DCFH, then trapped inside the cells. After washing the cells with PBS for three times, cells were collected by trypsinization. Then, the cells were suspended in PBS in order to take photos with an inverted fluorescence microscope (XD-202, Jiangnan Yongxin, China) and to assess fluorescence at an excitation wavelength of 488 nm and a emission wavelength of 525 nm with a flow cytometry (FACS Canto II, BD, USA).

Real-time polymerase chain reaction analysis of *CYP2E1*

Total RNA was obtained from treated BRL-3A cells with RNAiso Plus according to the instruction of the manufacturer. The quality and quantity of total RNA samples was determined using spectroscopic measurements at 260 and 280 nm. Samples used for subsequent studies had A_{260}/A_{280} ratios >1.8. The integrity of total RNA was checked by 1% agarose gel electrophoresis, and 28S, 18S, and 5.8S rRNAs were visualized after staining.[18] 2 μL RNA was used in a 20 μL reaction mixture utilizing Primescipt™ RT reagent kit according to the supplier's instructions. The primers used in these studies are shown in Table 1. Gene expression levels were measured by real-time PCR on a CFX96 real-time PCR system (Bio-Rad, USA). Reactions were performed in a final volume of 25 μL that contained 12.5 μL mix, 2 μL cDNA, 0.5 μL each of specific oligonucleotide primer (10 μM), and 9.5 μL DEPC-treated autoclaved distilled water. The cycling parameters were carried out using initial denaturation at 95°C for 10 min, followed by 40 cycles of denaturation at 95°C for 25 s, annealing at 55°C for 30 s, extension at 72°C for 50 s and final extension at 72°C for 10 min. The $2^{-\Delta\Delta Ct}$ method was

Table 1: Primer sequences and the fragment size

Target gene	Primer sequences (5'-3')	Fragment size
CYP2E1	F: TCTGCTCCTGTCTGCTATTCTG R: GATACTGCCAAAGCCAACTGT	100 bp
β-actin	F: GAGACCTTCAACACCCCAGCC R: AATGTCACGCACGATTTCCC	263 bp

used to calculate the expression levels of CYP2E1 mRNA relative to the internal control.[19]

Western blot analysis of CYP2E1

Treated BRL-3A cells were washed in PBS and scrapped into 30 μL RIPA lysis buffer, which contained 0.1 mM PMSF. Protein content was determined using the BCA protein assay kit. Proteins were subjected to SDS-PAGE and then transferred onto 0.45 μm nitrocellulose membrane. After blocking with 5% (w/v) skimmed milk solution for 1 h at room temperature to reduce nonspecific binding, the membranes were applied with antibodies against CYP2E1 (1:1000) and GAPDH (1:1000) overnight at 4°C, and followed by incubation with anti-rabbit IgG-HRP antibody (1:8000) for 1 h at room temperature, the antibodies were all diluted in 5% (w/v) skimmed milk solution. ECL western blotting substrate was used as the chemiluminescent substrate. The blot was developed using Kodak films and with intensifying screen.[18] The images were subjected to densitometry analysis using Gel Doc™ XR + System (Bio-Rad, USA).

Statistical analysis

All data were described as mean ± standard error of the mean of multiple independent experiments. Statistics were analyzed using one-way ANOVA followed by multiple comparisons with Dunnett's test (SPSS software). $P < 0.05$ or $P < 0.01$ was used to denote as statistically significant or statistically very significant, respectively.

RESULTS AND DISCUSSIONS

Cell viability was measured using the MTT assay and was shown to decrease in a concentration-dependent manner, treated by TAA for 2 h. Viability of BRL-3A cells was significantly reduced to 52.0% ± 2.2% at the concentration of 0.18 mol/L [Figure 2a]. This concentration of TAA was chosen to establish BRL-3A cells oxidative stress model, respectively. Cytotoxicity for different doses of CG (5, 10, 20, 40, 60, 80, 100 mg/L) and Bifendate (1, 10, 20, 30, 40 mg/L) was assessed. There was no sign of cytotoxicity was observed in any CG group, however, cell viability was significantly reduced to 77.89 ± 3.9% at the bifendate concentration of 50 mg/L compared to the untreated control ($P < 0.01$) [Figure 2b and c]. The effects of different doses of CG on the viability of oxidative stressed cells were examined, as shown in Figure 2b. Cell viability increased as CG concentration increased, and the maximal proliferation was observed when the CG

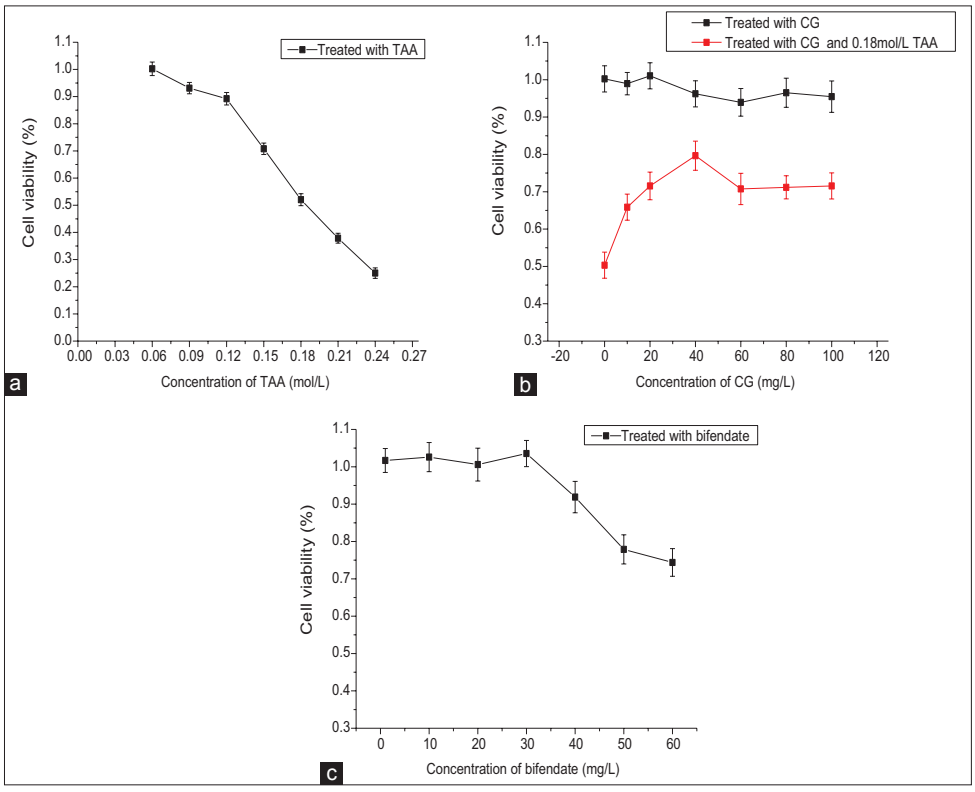

Figure 2: 3-[4,5-dimethylthiazol-2-yl]-2,5 diphenyl-tetrazolium bioassay ($n = 10$). (a) Concentration of thioacetamide to establish BRL-3A cells oxidative stress model. (b) Safe concentration of Calycosin-7-O-β-D-glucopyranoside (CG) and effects of CG on viability in oxidative stressed BRL-3A cells. (c) Safe concentration of bifendate on BRL-3A cells

concentration was 40 mg/L, while proliferation remained unchanged when the CG concentration was greater than 60 mg/L. Therefore, CG concentrations of 10 mg/L, 20 mg/L and 40 mg/L were selected for C1G, C2G and C3G, and the bifendate concentration of 40 mg/L was selected for PCG to do the following tests.

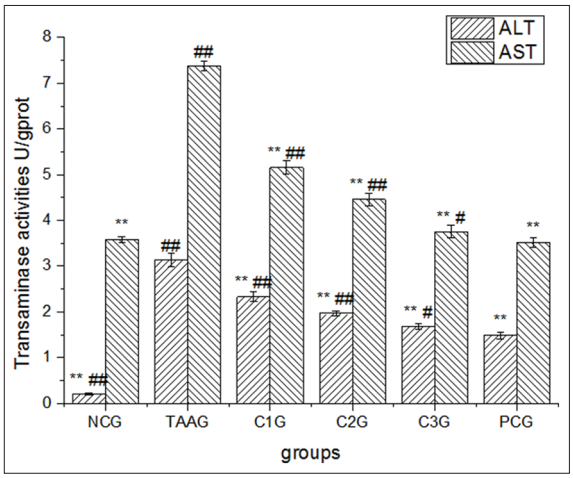

Figure 3: Effect of calycosin-7-O-β-D–glucopyranoside for transaminase activities in BRL-3A cell supernatants. Values are expressed as mean ± standard error of the mean, while $n = 3$. $^{*}P < 0.05$ compared to TAA groups (TAAG). $^{**}P < 0.01$ compared to TAAG. $^{\#}P < 0.05$ compared to PCG. $^{\#\#}P < 0.01$ compared to PCG

Both ALT and AST in TAAG that received 0.18 mol/L TAA treatment for 2 h showed significantly increase ($P < 0.01$), which indicated cell damage. Both ALT and AST in different CG groups and positive control group showed significantly decrease ($P < 0.01$), which indicated CG or bifendate all could reduce the aminotransferase activities of the oxidative stress cells. Both ALT and AST in C1G and C2G were significantly higher than PCG ($P < 0.01$), while in C3G they were significantly higher than PCG ($P < 0.05$). The results indicated that effect of bifendate was best in terms of reducing aminotransferase while it of C3G was nearest to PCG [Figure 3].

The treatment with TAA induced the amount of MDA as compared to negative control (NCG) as clear from Figure 4a. Compared to TAAG, both CG and bifendate were effective in reducing the amount of MDA ($P < 0.01$), meanwhile, the medium and high doses of CG had a better effect than bifendate ($P < 0.05$). Compared with NCG, T-AOC in TAAG was significantly decreased ($P < 0.01$), while it was improved in three doses of CG groups in a dose-dependent manner. As a result, T-AOC in C2G and C3G were significantly higher than it in PCG ($P < 0.01$) [Figure 4b]. It was found that the activity of SOD in TAAG was significantly decreased compared

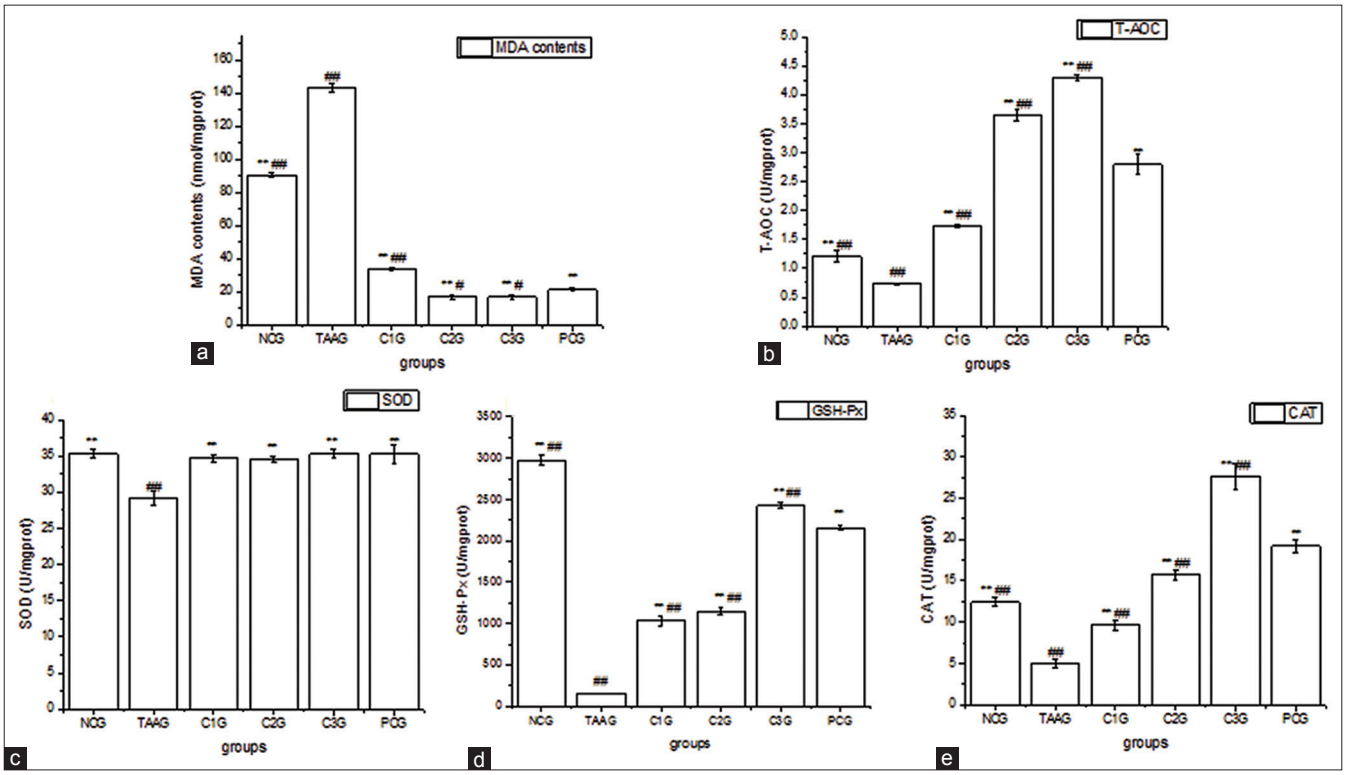

Figure 4: Effect of calycosin-7-O-β-D-glucopyranoside for antioxidant profiles and lipid peroxidation in BRL-3A cell. Values are expressed as Mean ± standard error of the mean, while $n = 3$. $^{*}P < 0.05$ compared to TAA group (TAAG). $^{**}P < 0.01$ compared to TAAG. $^{\#}P < 0.05$ compared to PCG. $^{\#\#}P < 0.01$ compared to PCG. (a) Effect of Calycosin-7-O-β-D-glucopyranoside (CG) for malondialdehyde in BRL-3A cells. (b) Effect of CG for total antioxidant capacity in BRL-3A cells. (c) Effect of CG for superoxide dismutase in BRL-3A cells. D. Effect of CG for glutathione peroxidase in BRL-3A cells. (e) Effect of CG for catalase in BRL-3A cells

with NCG ($P < 0.01$), and it in both CG groups and PCG was all significantly increased ($P < 0.01$). However, the effects of three doses of CG had no significantly different with bifendate ($P > 0.05$) [Figure 4c]. As shown in Figure 4d, the activity of GSH-Px in TAAG was significantly decreased compared with NCG ($P < 0.01$), meanwhile, both CG and bifendate had the abilities to make the dropped GSH-Px activity increased significantly again ($P < 0.01$), and C3G was higher than PCG ($P < 0.01$). Compared with NCG, the activity of CAT in TAAG was significantly decreased ($P < 0.01$), while it ascended in three doses of CG groups in a dose-dependent manner, and C3G was higher than PCG ($P < 0.01$) [Figure 4e].

Compared to NCG, the fluorescent signals generated with DCF-DA in TAAG were increased significantly with the observed period, while they were decreased in three doses of CG groups and bifendate group [Figure 5a]. Flow cytometry test results confirmed the observations from the fluorescence microscope [Figure 5b]. The maximum ROS levels were found in TAAG, which was 4.87 times higher than that in NCG. However, compared to TAAG, ROS levels were decreased in three doses of CG groups and bifendate group, but the data showed no significantly different between the four experimental groups ($P > 0.05$) [Figure 5c].

To assess the expression of *CYP2E1* mRNA and protein, real-time PCR and western blot analysis were performed using total RNA and protein isolated from the BRL-3A cells. As shown in Figure 6a, compared with NCG, the mRNA expression level of *CYP2E1* in TAAG was significantly increased to 2.26 times, while they in three doses of CG groups and bifendate group were significantly decreased ($P < 0.01$, compared with TAAG). Almost no differences were observed between C2G, C3G and PCG, which suggested both CG and bifendate could down regulate *CYP2E1* gene expression in oxidative stress BRL-3A cells, and the medium and high doses of CG had an equivalent effect to bifendate ($P > 0.05$).

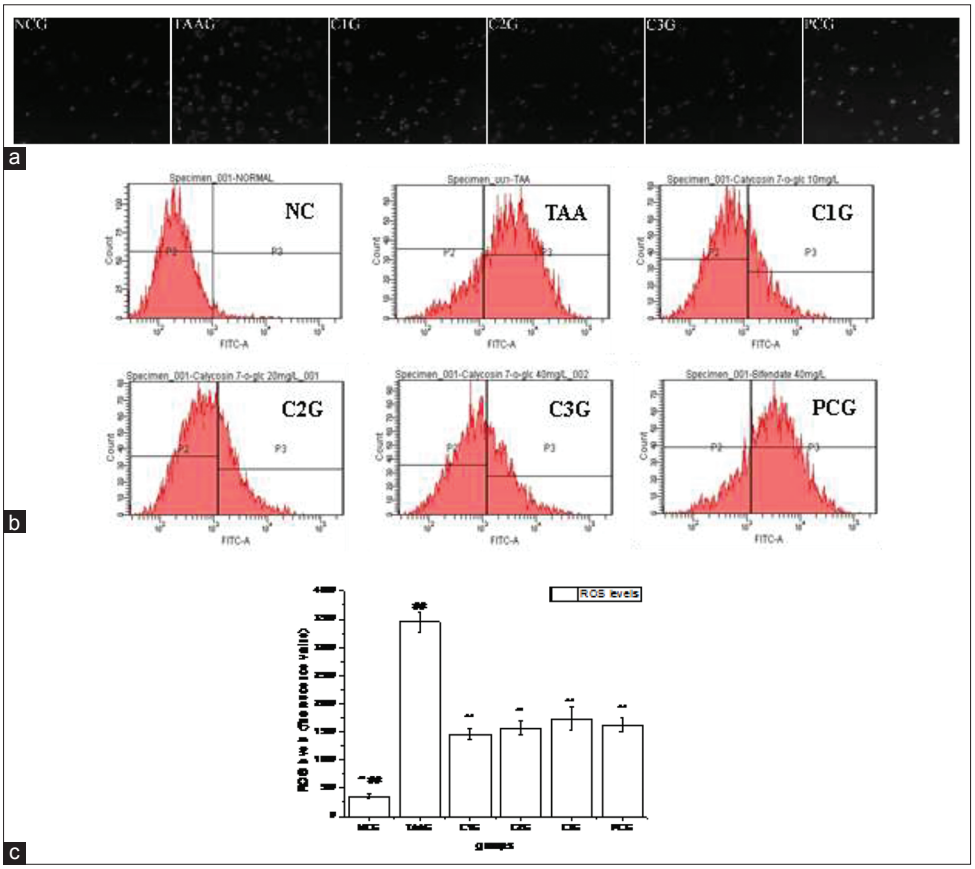

Figure 5: Effects of Calycosin-7-O-β-D-glucopyranoside on intracellular reactive oxygen species (ROS) production against oxidative stress of BRL-3A cell induced by thioacetamide. Values are expressed as mean ± standard error of the mean, while $n = 3$. *$P < 0.05$ compared to TAA group (TAAG). **$P < 0.01$ compared to TAAG. #$P < 0.05$ compared to PCG. ##$P < 0.01$ compared to PCG. (a) Representative images of ROS generation probed with dichlorofluorescein diacetate (DCF-DA) were obtained by fluorescence microscope. (b) ROS generation probed with dichlorofluorescein diacetate (DCF-DA) was obtained by flow cytometry. (c) Effect of Calycosin-7-O-β-D-glucopyranoside for ROS generation in BRL-3A cells analysed from flow cytometry images

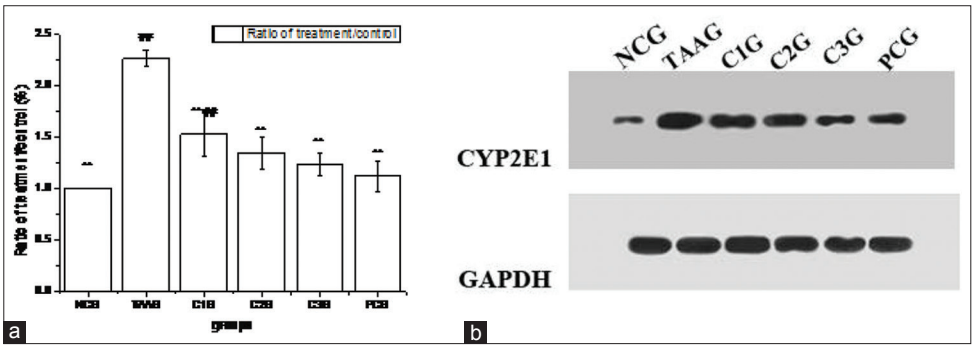

Figure 6: Effects of Calycosin-7-O-β-D-glucopyranoside on CYP2E1 expression against oxidative stress of BRL-3A cell induced by thioacetamide. Values are expressed as mean ± standard error of the mean, while $n = 3$. $^{*}P < 0.05$ compared to TAA group (TAAG). $^{**}P < 0.01$ compared to TAAG. $^{\#}P < 0.05$ compared to PCG. $^{\#\#}P < 0.01$ compared to PCG. (a) Result of real-time PCR assay, (b) Western blot assay

The Western blot for CYP2E1 showed a similar result to the real-time PCR analysis, which was shown in Figure 6b. Compared with NCG, the protein expression level of CYP2E1 in TAAG was significantly increased to 6.23 times. While CG could down regulate the increased CYP2E1 protein levels in a dose-dependent manner, and high dose of CG had an equivalent effect to bifendate.

Liver plays the main role in the metabolism of different nutrients, such as carbohydrates, proteins, and lipids; in addition, it shares in clearance of waste products resulting from metabolism and elimination of exogenous drugs and other xenobioc.[20] Currently, liver cells models *in vitro* for oxidative damage are mainly stellate Cell[21] or embryonic liver cell line.[22] However, these models cannot reflect the variation of metabolism in the liver precisely, because the main cell type that constitutes liver is parenchymal cells. The BRL 3A immortal rat liver cell line, which is a kind of parenchymal cells, is selected in the present study as a convenient *in vitro* model to assess nanocellular toxicity. This cell line has been well characterized for its relevance to toxicity models.[23] Aim of this study is to investigate the effects and mechanism for CG protecting BRL-3A cells undergone oxidative stress.

Thioacetamide is well-known to induce both acute and chronic hepatic failure,[24-26] and is widely applied to develop animal models of centrilobular necrosis in the liver,[27,28] cirrhosis in rats,[29] fibrosis[30] and hepatic encephalopathy.[31] TAA is metabolized in the liver by flavin containing monozygenase (mixed function oxidase system) and finally becomes TAA-S-oxide metabolite (TASO).[32] TASO is subsequently transformed into TAA S, S-dioxide with or without being further oxidized to form species that exert their toxic effect on several organs, including plasma, liver, kidney, bone marrow, adrenals, and other tissues. TAA undergoes an extensive metabolism to acetate, and it is finally excreted through the urine within 24 h.[33] It was described that the mechanism of TAA hepatotoxicity may be that TAA acts as creator of ROS leading to lipid peroxidation, oxidation of cellular proteins and extensive mitochondrial DNA strand breakage, thus inducing impairment of mitochondrial protein synthesis.[34]

It is well recognized that cellular antioxdant enzymes, which can restrict production of ROS are essential with regards to defending the liver cells from toxin-induced damage. Meanwhile, lipid peroxidation has an important role in the etiology of injury caused by oxidative stress, as lipids are an important part of biological membranes and due to the presence of double bonds are susceptible to the attack of ROS.[35] Whereas, various plant components were found to increase the endogenous anti-oxidant enzymes SOD, CAT and GSH-Px and inhibit lipid peroxidation under oxidative stress.[36,37] And some components of *Astragalus* also had the similar effect.[38] However, as another major medicinal ingredient in *Astragalus*, it is not yet clear that whether CG had these effects.

This research revealed that TAA triggered ROS overproduction and decreased the cellular T-AOC and anti-oxidant enzymes SOD, CAT and GSH-Px, meanwhile increased the MDA in the BRL-3A cells. The data further showed that T-AOC, SOD, CAT and GSH-Px depletion due to TAA was recovered and the elevated level of MDA was also reduced when the damaged cells were treated with CG [Figure 4]. Moreover, the test results indicated that CG had the effect to reduce the high ROS levels directly caused by TAA [Figure 5]. Parallel findings were consistent with our study, which showed that *Curcuma longa* possessed protective effect against TAA.[39]

Lately, it is found that TAA is metabolized by CYP2E1 enzymes in liver microsomes and is transformed to ROS.[40] However, there are only a few *in vivo* studies about the effect of CYP2E1 on oxidative stress induced by TAA

and little is known about the *in vitro* effects. Therefore, it is important to determine the influence of CG on CYP2E1 *in vitro*, especially in liver parenchymal cells. In this study, the mRNA and protein expression level of *CYP2E1* in BRL-3A cells were measured, and both of them were significantly increased with TAA treatment, and were recovered when the injured cells were treated with CG [Figure 6]. The inhibiting effect of CG to CYP2E1 may be one of the significant factors in hepatoprotective activity by inhibiting the metabolism of TAA and blocking the release of ROS that is responsible for inducing damage of hepatocytes.

REFERENCES

1. Dubey N, Khan AM, Raina R. Sub-acute deltamethrin and fluoride toxicity induced hepatic oxidative stress and biochemical alterations in rats. Bull Environ Contam Toxicol 2013;91:334-8.
2. Kim JH, Qu A, Reddy JK, Gao B, Gonzalez FJ. Hepatic oxidative stress activates the *Gadd45b* gene by way of degradation of the transcriptional repressor STAT3. Hepatology 2014;59:695-704.
3. National Pharmacopoeia Committee. Pharmacopoeia of the People's Republic of China. 2010 ed., Vol. I. Beijing: Chinese Medicine Science and Technology Press; 2010. p. 283-4.
4. Auyeung KK, Cho CH, Ko JK. A novel anticancer effect of *Astragalus* saponins: Transcriptional activation of NSAID-activated gene. Int J Cancer 2009;125:1082-91.
5. Yuan X, Sun S, Wang S, Sun Y. Effects of Astragaloside IV on IFN-gamma level and prolonged airway dysfunction in a murine model of chronic asthma. Planta Med 2011;77:328-33.
6. Liu H, Wei W, Sun WY, Li X. Protective effects of Astragaloside IV on porcine-serum-induced hepatic fibrosis in rats and *in vitro* effects on hepatic stellate cells. J Ethnopharmacol 2009;122:502-8.
7. Wang C, Xu YQ. Diphenyl dimethyl bicarboxylate in the treatment of viral hepatitis, adjuvant or curative? Gastroenterol Res 2008;1:2-7.
8. Das J, Ghosh J, Manna P, Sil PC. Acetaminophen induced acute liver failure via oxidative stress and JNK activation: Protective role of taurine by the suppression of cytochrome P450 2E1. Free Radic Res 2010;44:340-55.
9. Mosmann T. Rapid colorimetric assay for cellular growth and survival: Application to proliferation and cytotoxicity assays. J Immunol Methods 1983;65:55-63.
10. Reitman S, Frankel S. A colorimetric method for the determination of serum glutamic oxalacetic and glutamic pyruvic transaminases. Am J Clin Pathol 1957;28:56-63.
11. Bradford MM. A rapid and sensitive method for the quantitation of microgram quantities of protein utilizing the principle of protein-dye binding. Anal Biochem 1976;72:248-54.
12. Benzie IF, Strain JJ. The ferric reducing ability of plasma (FRAP) as a measure of "antioxidant power": The FRAP assay. Anal Biochem 1996;239:70-6.
13. Ohkawa H, Ohishi N, Yagi K. Assay for lipid peroxides in animal tissues by thiobarbituric acid reaction. Anal Biochem 1979;95:351-8.
14. Polavarapu R, Spitz DR, Sim JE, Follansbee MH, Oberley LW, Rahemtulla A, *et al.* Increased lipid peroxidation and impaired antioxidant enzyme function is associated with pathological liver injury in experimental alcoholic liver disease in rats fed diets high in corn oil and fish oil. Hepatology 1998;27:1317-23.
15. Yand QM, Pan XH, Kong WB, Yang H, Su YD, Zhang L, *et al*. Antioxidant activities of malt extract from barley (*Hordeum vulgare* L.) toward various oxidative stress *in vitro* and *in vivo*. Food Chem 2010;118:84-9.
16. Beers RF Jr, Sizer IW. A spectrophotometric method for measuring the breakdown of hydrogen peroxide by catalase. J Biol Chem 1952;195:133-40.
17. Rothe G, Valet G. Flow cytometric analysis of respiratory burst activity in phagocytes with hydroethidine and 2-7-dichlorofluorescin. J Leukoc Biol 1990;47:440-8.
18. Zhong Y, Dong G, Luo H, Cao J, Wang C, Wu J, *et al.* Induction of brain CYP2E1 by chronic ethanol treatment and related oxidative stress in hippocampus, cerebellum, and brainstem. Toxicology 2012;302:275-84.
19. Seth RK, Das S, Kumar A, Chanda A, Kadiiska MB, Michelotti G, *et al.* CYP2E1-dependent and leptin-mediated hepatic CD57 expression on CD8+T cells aid progression of environment-linked nonalcoholic steatohepatitis. Toxicol Appl Pharmacol 2014;274:42-54.
20. Yiran Z, Chenyang J, Jiajing W, Yan Y, Jianhong G, Jianchun B, *et al.* Oxidative stress and mitogen-activated protein kinase pathways involved in cadmium-induced BRL 3A cell apoptosis. Oxid Med Cell Longev 2013;2013:516051.
21. Nakamura I, Zakharia K, Banini BA, Mikhail DS, Kim TH, Yang JD, *et al.* Brivanib attenuates hepatic fibrosis *in vivo* and stellate cell activation *in vitro* by inhibition of FGF, VEGF and PDGF signaling. PLoS One 2014;9:e92273.
22. Salama SM, AlRashdi AS, Abdulla MA, Hassandarvish P, Bilgen M. Protective activity of panduratin A against thioacetamide-induced oxidative damage: Demonstration with *in vitro* experiments using WRL-68 liver cell line. BMC Complement Altern Med 2013;13:279.
23. Boess F, Kamber M, Romer S, Gasser R, Muller D, Albertini S, *et al.* Gene expression in two hepatic cell lines, cultured primary hepatocytes, and liver slices compared to the *in vivo* liver gene expression in rats: Possible implications for toxicogenomics use of *in vitro* systems. Toxicol Sci 2003;73:386-402.
24. Ishikawa S, Ikejima K, Yamagata H, Aoyama T, Kon K, Arai K, *et al.* CD1d-restricted natural killer T cells contribute to hepatic inflammation and fibrogenesis in mice. J Hepatol 2011;54:1195-204.
25. Steib CJ, Hennenberg M, Beitinger F, Hartmann AC, Bystron M, De Toni EN, *et al.* Amiloride reduces portal hypertension in rat liver cirrhosis. Gut 2010;59:827-36.
26. Zaldivar MM, Pauels K, von Hundelshausen P, Berres ML, Schmitz P, Bornemann J, *et al.* CXC chemokine ligand 4 (Cxcl4) is a platelet-derived mediator of experimental liver fibrosis. Hepatology 2010;51:1345-53.
27. Chilakapati J, Shankar K, Korrapati MC, Hill RA, Mehendale HM. Saturation toxicokinetics of thioacetamide: Role in initiation of liver injury. Drug Metab Dispos 2005;33:1877-85.
28. Fujisawa K, Miyoshi T, Tonomura Y, Izawa T, Kuwamura M, Torii M, *et al.* Relationship of heat shock protein 25 with reactive macrophages in thioacetamide-induced rat liver injury. Exp Toxicol Pathol 2011;63:599-605.
29. Ide M, Yamate J, Machida Y, Sawamoto O, Nakanishi M, Kuwamura M, *et al.* Macrophage populations, myofibroblastic cells, and extracellular matrix accumulation in chronically-developing rat liver cirrhosis induced by repeated injection of thioacetamide. J Toxicol Pathol 2002;15:19-29.
30. Bruck R, Aeed H, Shirin H, Matas Z, Zaidel L, Avni Y, *et al.* The hydroxyl radical scavengers dimethylsulfoxide and dimethylthiourea protect rats against thioacetamide-induced fulminant hepatic failure. J Hepatol 1999;31:27-38.
31. Avraham Y, Israeli E, Gabbay E, Okun A, Zolotarev O, Silberman I, *et al.* Endocannabinoids affect neurological and cognitive

function in thioacetamide-induced hepatic encephalopathy in mice. Neurobiol Dis 2006;21:237-45.

32. Chen S, Wang HT, Yang B, Fu YR, Ou QJ. Protective effects of recombinant human growth hormone on cirrhotic rats. World J Gastroenterol 2004;10:2894-7.
33. Spira B, Raw I. The effect of thioacetamide on the activity and expression of cytosolic rat liver glutathione-S-transferase. Mol Cell Biochem 2000;211:103-10.
34. Lewis W, Copeland WC, Day BJ. Mitochondrial DNA depletion, oxidative stress, and mutation: Mechanisms of dysfunction from nucleoside reverse transcriptase inhibitors. Lab Invest 2001;81:777-90.
35. Kadir FA, Kassim NM, Abdulla MA, Yehye WA. Effect of oral administration of ethanolic extract of *Vitex negundo* on thioacetamide-induced nephrotoxicity in rats. BMC Complement Altern Med 2013;13:294.
36. Wang Y, Zhu H, Tam NF. Effect of a polybrominated diphenyl ether congener (BDE-47) on growth and antioxidative enzymes of two mangrove plant species, *Kandelia obovata* and *Avicennia marina*, in South China. Mar Pollut Bull 2014;85:376-84.
37. Tian Y, Zou B, Yang L, Xu SF, Yang J, Yao P, *et al*. High molecular weight persimmon tannin is a potent hypolipidemic in high-cholesterol diet fed rats. Food Res Int 2012;48:970-7.
38. Wu X, Hu J. Pretreatment with astragaloside IV protects H9c2 cells against hydrogen peroxide-induced apoptosis by scavenging of reactive oxygen species and regulation of Bcl-2 and Bax expression. J Med Plants Res 2011;5:3304-11.
39. Salama SM, Abdulla MA, AlRashdi AS, Ismail S, Alkiyumi SS, Golbabapour S. Hepatoprotective effect of ethanolic extract of *Curcuma longa* on thioacetamide induced liver cirrhosis in rats. BMC Complement Altern Med 2013;13:56.
40. Kadir FA, Othman F, Abdulla MA, Hussan F, Hassandarvish P. Effect of *Tinospora crispa* on thioacetamide-induced liver cirrhosis in rats. Indian J Pharmacol 2011;43:64-8.

Cite this article as: Jian L, Xin L, Yufang M, Yifan H. Protective effect of calycosin-7-O-β-D-glucopyranoside against oxidative stress of BRL-3A cells induced by thioacetamide. Phcog Mag 2015;11:524-32.

Source of Support: Nil, **Conflict of Interest:** None declared.